Lower hybrid instability in a tokamak under neutral beam injection and magnetic shear

Animesh Kuley[a] and V. K. Tripathi
Department of Physics, Indian Institute of Technology Delhi, New Delhi 110016, India

(Received 13 November 2007; accepted 31 March 2008; published online 22 May 2008)

A slab model is developed to study the excitation of lower hybrid instability triggered by the injection of a transverse neutral beam in a tokamak with magnetic shear. The lower hybrid mode is evanescent in the inner and outer region while propagating waves in the intermediate region. The neutral beam, on getting fully ionized in the plasma, resonantly couples with the lower hybrid wave in the intermediate region, driving the mode unstable. The theory of this process reveals that the growth rate scales as one third power of beam density, and increases significantly with the sheared magnetic field due to modification in the parallel wave number and the mode structure. © *2008 American Institute of Physics*. [DOI: 10.1063/1.2912460]

I. INTRODUCTION

Microinstabilities driven by ion velocity distributions play an important role in fusion plasma. A number of experimental observations of instabilities driven by neutral beams and fusion products have been reported for Japan Torus (JT-60),[1] Joint European Torus (JET),[2–5] Wendelstein 7-AS (W7-AS),[6] Tokamak Fusion Test Reactor (TFTR),[7] and smaller devices.[8–11] The spatial dependence of the deposition of the beam power inside the plasma is determined by ionization cross section of the neutral beam and the plasma electron density profile. The ionization of the injected beam and the charge-exchange between plasma ions and neutrals produce ions with the same energy and direction of motion as atoms in the original neutral beam. Fast ions are seen to be lost due to vertical ∇B-drift and interaction with magnetohydrodynamics (MHD) and other instabilities. Shalashov *et al.* have experimentally observed the effect of fast ion confinement on lower hybrid (LH) wave excitation in the W7-AS stellarator.[6] Baldzuhn *et al.* have observed that the fast ion losses are much stronger during the perpendicular neutral beam injection, while the global energy confinement is much higher than the tangential neutral beam injection.[12] Neutral beam offers the flexibility of being able to heat the hydrogen plasma envisaged during the initial phases of the International Thermonuclear Experimental Reactor (ITER) operation by using beams of hydrogen atoms. During the D and DT phases in the thermonuclear ignition and burn control scenarios, the injector would supply up to 50 MW of deuterium beams at 1 MeV.[13]

Recent experiments in W7-AS,[6] reported two instabilities triggered by the injection of the quasitransverse hydrogen beam. First, a lower hybrid instability when lower hybrid frequency coincides with a high ion cyclotron harmonic. Second, a kinetic instability of ion Bernstein wave at ion cyclotron harmonics, lower than the lower hybrid frequency. An instability at the second harmonic ion cyclotron frequency was observed in the JT-60 tokamak with the injection of high power perpendicular neutral beams.[1] High power ion heating was observed experimentally with perpendicular neutral beam injection, which improved the mode of ion transport, anomalous transport, and enhanced toroidal flow in the core region of the Large Helical Device (LHD) by Nagaoka *et al.*[14] It has often been observed that high power neutral beam injection (NBI), both tangentially and perpendicularly to the magnetic field, causes a fishbonelike instability in which strong sawtoothlike bursts destroy the plasma stability.[15,16] In fact ion cyclotron harmonic waves, as well as the fishbone instability were observed in the Poloidal-Divertor Experiment (PDX) tokamak with perpendicular neutral beam injection.[16,17] A number of theoretical models have been proposed for explaining the beam driven fishbone instabilities.[18–21] Rosenberg *et al.* investigated lower hybrid instability in a collisionless dusty magnetized plasma driven by a negatively charge dust beam streaming across a magnetic field.[22]

In this paper we develop a theory for the lower hybrid instability triggered by the injection of a transverse neutral beam in a tokamak. We model the plasma by a slab geometry and retain the effect of finite magnetic shear. We employ the fluid theory to obtain tractable dispersion relation and eigenfunctions.

In Sec. II we elaborate on the physical model and carry out the stability analysis. The results and discussions are given in Sec. III.

II. PHYSICAL MODEL AND STABILITY ANALYSIS

We model the tokamak by a plasma slab with uniform electron density n_0 placed in a sheared magnetic field $\mathbf{B}=B_0[\hat{z}+(\alpha x/a)\hat{y}]$, where a is the plasma minor radius, and α is the shear parameter.[23–26] The x, y, and z directions in the slab geometry correspond to radial, poloidal, and toroidal directions in the tokamak configuration. A neutral beam with velocity $v_{0b}\hat{y}$, density n_{0b} propagates through the plasma. The beam quickly turns into an ion beam of charge e and mass M. We perturb the equilibrium by lower hybrid wave perturbation of electrostatic potential

[a]Electronic mail: animesh.kuley@mail2.iitd.ac.in.

$$\phi = \phi(x) e^{-i(\omega t - k_y y - k_z z)}, \tag{1}$$

where ω lies in the range $\omega_{ci} \ll \omega \ll \omega_{ce}$, and $k_\perp \rho_e \ll 1$, where ω_{ci} and ω_{ce} are the ion and electron cyclotron frequencies and ρ_e is the electron Larmor radius. In this limit the ion motion can be taken to be unmagnetized and one may employ the fluid equation for the electron response. The linearized equations of motion and continuity for perturbed electrons velocity v and density n can be written as

$$m\frac{\partial v}{\partial t} = e\nabla\phi - e\mathrm{v}\times\mathrm{B},$$
$$\frac{\partial n}{\partial t} + \nabla\cdot(n_0 \mathrm{v}) = 0. \tag{2}$$

Expressing $\nabla\phi = \nabla_\perp\phi + 1/B(B\cdot\nabla)$, where $\nabla_\perp$ is the component of ∇ perpendicular to the magnetic field, and replacing $\partial/\partial t$ by $-i\omega$ in these equations and solving them, we obtain

$$v_{1\perp} = \frac{e}{m}\frac{\nabla_\perp\phi\times\boldsymbol{\omega}'_{ce} + i\omega\nabla_\perp\phi}{\omega^2 - \omega'^2_{ce}},$$
$$v_{1\parallel} = -\frac{e}{mi\omega}\nabla_\parallel\phi, \tag{3}$$
$$n_{1e} = \frac{n_0 e}{m}\left[\frac{\nabla^2_\parallel\phi}{\omega^2} - \frac{\nabla^2_\perp\phi}{\omega'^2_{ce}}\right],$$

where $\boldsymbol{\omega}'_c = \omega_{ce}[\hat{z} + (\alpha x/a)\hat{y}]$, $\omega_{ce} = eB_0/m$, $-e$, m, and ω_{ce} are the electron charge, mass, and electron cyclotron frequency and subscript 1 refers to perturbed quantities.

By assuming the response of the plasma ions to be unmagnetized, the perturbed ion density can be written as

$$n_{1i} = -\frac{n_{0i}e}{m_i\omega^2}\nabla^2\phi, \tag{4}$$

where e, m_i, and n_{0i} are the ion charge, mass, and equilibrium density, respectively.

By assuming the response of the ion beam to be unmagnetized, on solving the linearized equations of motion and continuity turns out to be

$$v_{1b} = \frac{e\nabla\phi}{Mi(\omega - k_y v_{0b})},$$
$$n_{1b} = -\frac{n_{0b}e}{M}\frac{\nabla^2\phi}{(\omega - k_y v_{0b})^2}. \tag{5}$$

Using Eqs. (3)–(5) in the Poisson equation, $\nabla^2\phi = 4\pi e(n_{1e} - n_{1i} - n_{1b})$, we get

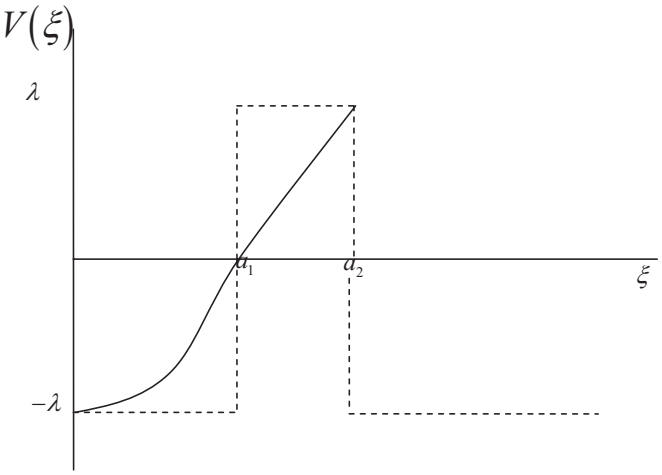

FIG. 1. Variation of $V(\xi) = -\lambda + \xi^2$ with ξ and a suitable model profile.

$$\nabla^2_\perp\phi + \frac{\frac{\omega^2_{pi}}{\omega^2} + \frac{\omega^2_p}{\omega^2} - 1}{1 - \frac{\omega^2_{pi}}{\omega^2} + \frac{\omega^2_p}{\omega^2_{ce}}}\left(k_y^2\alpha^2\frac{x^2}{a^2} + 2k_z k_y \alpha\frac{x}{a} + k_z^2\right)\phi$$
$$= -\frac{\omega^2_{pb}k_y^2}{(\omega - k_y v_{0b})^2\left[1 - \frac{\omega^2_{pi}}{\omega^2} + \frac{\omega^2_p}{\omega^2_{ce}}\right]}\phi. \tag{6}$$

Inside the parentheses on the left-hand side of Eq. (6) we may neglect last two terms compared to the first one as k_z is small. Introducing a dimensionless variable $\xi = x/\beta$, where $\beta^4 = a^2/\alpha^2 k_y^2[1 + \omega^2_{pi}/\omega^2 + \omega^2_p/\omega^2 - 1/1 - \omega^2_{pi}/\omega^2 + \omega^2_p/\omega^2_{ce}]$, one may rewrite Eq. (6) as

$$\frac{d^2\phi}{d\xi^2} + [-\lambda + \xi^2]\phi = -\frac{\omega^2_{pb}k_y^2\beta^2}{(\omega - k_y v_{0b})^2\left[1 - \frac{\omega^2_{pi}}{\omega^2} + \frac{\omega^2_p}{\omega^2_{ce}}\right]}\phi, \tag{7}$$

where

$$\lambda = (k_y^2 + k_z^2)\beta^2. \tag{8}$$

In the absence of the beam, Eq. (7) takes the form

$$\frac{d^2\phi}{d\xi^2} + V(\xi)\phi = 0, \tag{9}$$

where $V(\xi) = -\lambda + \xi^2$, is shown in Fig. 1. $V(\xi)$, has a turning point at $\xi = \sqrt{\lambda}$. For $\xi < \sqrt{\lambda}$, $V(\xi)$ is $-ve$ and the wave is evanescent. For $\xi > \sqrt{\lambda}$, $V(\xi)$ is $+ve$ and ϕ is a propagating wave. Outside the plasma again the wave is evanescent. Thus to solve Eq. (9) we model the $V(\xi)$ profile as follows:

$$V(\xi) = -\lambda \quad \text{for } 0 < \xi < a_1 \text{ (region I)}$$
$$= \lambda \quad \text{for } a_1 < \xi < a_2 \text{ (region II)} \tag{10}$$
$$= -\lambda \quad \text{for } \xi > a_2 \text{ (outside region)},$$

where $a_1 = \sqrt{\lambda}$, and we may choose $a_2 = a_1\sqrt{2}$.

The solution of Eq. (9) can be written as

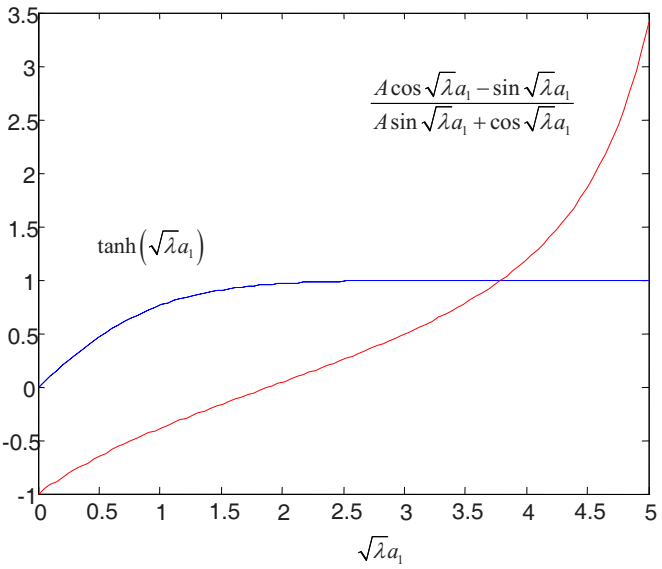

FIG. 2. (Color online) Graphical solution of transcendental of Eq. (14). The point of intersection gives the root $\lambda=\lambda_0$.

$$\phi_{\mathrm{I}} = C_1[e^{\sqrt{\lambda}\xi} + e^{-\sqrt{\lambda}\xi}] \quad \text{for} \quad 0 < \xi < a_1, \tag{11}$$

$$\phi_{\mathrm{II}} = C_2 \sin\sqrt{\lambda}\xi + C_3 \cos\sqrt{\lambda}\xi \quad \text{for} \quad a_1 < \xi < a_2, \tag{12}$$

$$\phi_{\mathrm{III}} = C_4 e^{-\sqrt{\lambda}\xi} \quad \text{(outside region)}, \tag{13}$$

where C_1, C_2, C_3, and C_4 are the constants of integration.

Employing the continuity of ϕ and its first derivative at $\xi=a_1,a_2$ we get the dispersion relation

$$\tanh(\sqrt{\lambda}a_1) = \frac{A\cos\sqrt{\lambda}a_1 - \sin\sqrt{\lambda}a_1}{A\sin\sqrt{\lambda}a_1 + \cos\sqrt{\lambda}a_1}, \tag{14}$$

where

$$A = \frac{\sin\sqrt{\lambda}a_2 - \cos\sqrt{\lambda}a_2}{\sin\sqrt{\lambda}a_2 + \cos\sqrt{\lambda}a_2}, \quad \sqrt{\lambda}a_1 = \lambda.$$

We solve the above transcendental equation graphically by plotting the left-hand side (LHS) and right-hand side (RHS) as functions of $\sqrt{\lambda}a_1$ as shown in Fig. 2. The point of intersection where LHS=RHS gives the solution $\lambda=\lambda_0$ of Eq. (14). The wave functions of the eigenmode can be written as

$$\phi = \begin{cases} \phi_{\mathrm{I}} = RC_4[e^{\sqrt{\lambda_0}\xi} + e^{-\sqrt{\lambda_0}\xi}] & \text{for } 0 < \xi < a_1 \\ \phi_{\mathrm{II}} = PC_4[A\sin\sqrt{\lambda_0}\xi + \cos\sqrt{\lambda_0}\xi] & \text{for } a_1 < \xi < a_2 \\ \phi_{\mathrm{III}} = C_4 e^{-\sqrt{\lambda_0}\xi} & \text{for outside}, \end{cases} \tag{15}$$

where

$$P = \frac{e^{-\sqrt{2}\lambda_0}}{A\sin\sqrt{2}\lambda_0 + \cos\sqrt{2}\lambda_0}, \quad R = \frac{AP\sin\lambda_0 + P\cos\lambda_0}{e^{\lambda_0} + e^{-\lambda_0}}. \tag{16}$$

In terms of λ_0 the eigenfrequency of the lower hybrid mode turns out to be

$$\omega_0 = \left[\frac{(k_y^2a^2 + k_z^2a^2)^2\omega_{pi}^2 + \lambda_0^2\alpha^2k_y^2a^2\omega_p^2}{(k_y^2a^2 + k_z^2a^2)^2\left(1 + \frac{\omega_p^2}{\omega_{ce}^2}\right) - \lambda_0^2\alpha^2k_y^2a^2\frac{\omega_p^2}{\omega_{ce}^2}}\right]^{1/2}. \tag{17}$$

One may note that in the absence of shear ($\alpha=0$) the eigenfrequency reduces to $\omega=\omega_{\mathrm{LH}}=\omega_{pi}/(1+\omega_p^2/\omega_{ce}^2)^{1/2}$, i.e., the lower hybrid frequency. This is because we have neglected k_z^2 as compared to the shear term.

When the beam term is not zero, we may take ϕ to remain largely unmodified, however the eigenvalue changes,[27]

$$\frac{d^2\phi}{d\xi^2} + (-\lambda + \xi^2)\phi = -\frac{\omega_{pb}^2k_y^2\beta^2}{(\omega - k_yv_{0b})^2\left(1 - \frac{\omega_{pi}^2}{\omega_0^2} + \frac{\omega_p^2}{\omega_{ce}^2}\right)}\phi, \tag{18}$$

where we have taken $\omega=\omega_0$ in the nonresonant term on the RHS. For a beam launched from the transverse direction (y direction) its x or ξ profile may be taken as

$$\omega_{pb}^2 = \omega_{pbo}^2 \quad \text{for } a_1 < \xi < a_2,$$
$$= 0 \quad \text{otherwise}. \tag{19}$$

Further, since

$$\frac{d^2\phi}{d\xi^2} + (-\lambda_0 + \xi^2)\phi = 0, \tag{20}$$

by employing Eq. (20) in Eq. (18) and multiplying the resulting equation by $\phi^*d\xi$ and integrating over the entire domain we obtain

$$\lambda - \lambda_0 = -\frac{I_1\omega_{pbo}^2}{I_0(\omega - k_yv_{0b})^2}, \tag{21}$$

where

$$I_1 = \int_{a_1}^{a_2}\phi_{\mathrm{II}}^*\frac{\beta^2k_y^2}{\left(1 - \frac{\omega_{pi}^2}{\omega_0^2} + \frac{\omega_p^2}{\omega_{ce}^2}\right)}\phi_{\mathrm{II}}d\xi,$$
$$I_0 = \int_0^{\infty}\phi^*\phi d\xi. \tag{22}$$

Using the expression for λ from Eq. (8) one may rewrite Eq. (21) as

$$(\omega^2 - \omega_0^2)(\omega - k_yv_{0b})^2 = -b_2^2\omega_{pbo}^2\frac{I_1}{I_0}, \tag{23}$$

where

$$b_2^2 = \frac{2\lambda_0\alpha^2\left(\frac{\omega_p^2}{\omega_{ce}^2}\omega_0^2 + \omega_p^2\right)k_y^2a^2}{(k_y^2a^2 + k_z^2a^2)^2\left(1 + \frac{\omega_p^2}{\omega_{ce}^2}\right) - \lambda_0^2\alpha^2k_y^2a^2\frac{\omega_p^2}{\omega_{ce}^2}}. \tag{24}$$

Here $\omega\approx\omega_0$ corresponds to the lower hybrid mode in the absence of the beam, and $\omega\approx k_yv_{0b}$ is the beam mode. We are looking for solutions when $\omega_0\approx k_yv_{0b}$, i.e., when the

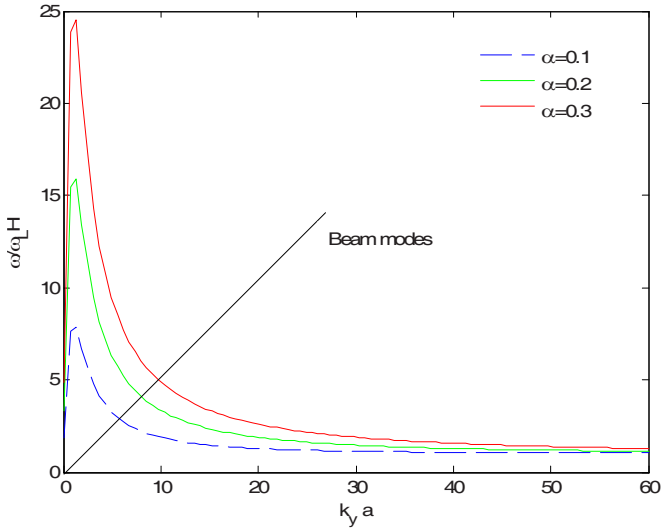

FIG. 3. (Color online) Dispersion curve for lower hybrid wave and beam modes with plasma density $\sim(2-6)\times10^{13}$ cm^{-3}, magnetic field 2.5 T, for different magnetic shear parameter $\alpha=0.1$, $\alpha=0.2$, and $\alpha=0.3$.

beam is in Cerenkov resonance with the lower hybrid mode. We expand ω as $\omega=\omega_0+\delta=k_y v_{0b}+\delta$, where δ is the modification in ω due to the finite right-hand side of Eq. (21). Then Eq. (23) takes the form $\delta^3=[(b_2^2\omega_{pb0}^2/2\omega_0)(I_1/I_0)]e^{i2l\Pi}$, $l=0,1,2$.

The growth rate of the unstable mode is

$$\gamma=\mathrm{Im}(\delta)=\frac{\sqrt{3}}{2}\left(\frac{b_2^2\omega_{pb0}^2}{2\omega_0}\frac{I_1}{I_0}\right)^{1/3}. \tag{25}$$

Growth rate varies as one third power of beam density. Equation (24) shows that b_2 depends on the spatial variation and shear parameter (α). It also shows that the growth rate vanishes when the shear parameter (α) goes to zero. However, the theory is not valid for the case of zero shear [cf. the approximation mentioned below Eq. (6)]. For finite α, the growth rate and localization of the mode are strongly dependent on α, the shear parameter.

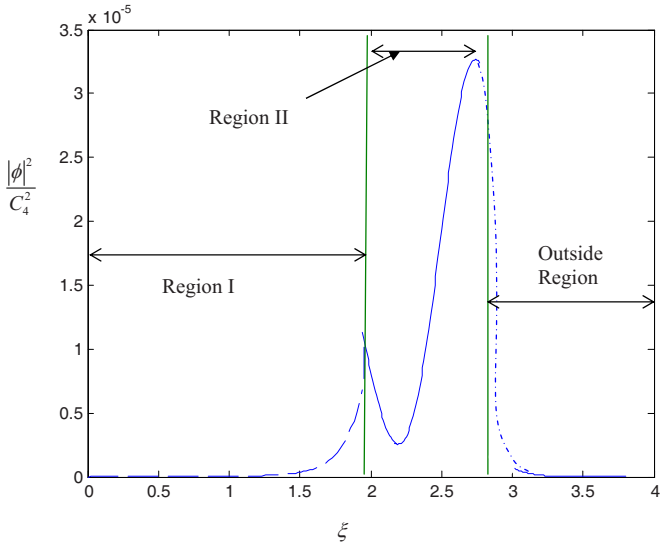

FIG. 4. (Color online) Probability distribution of the wave functions.

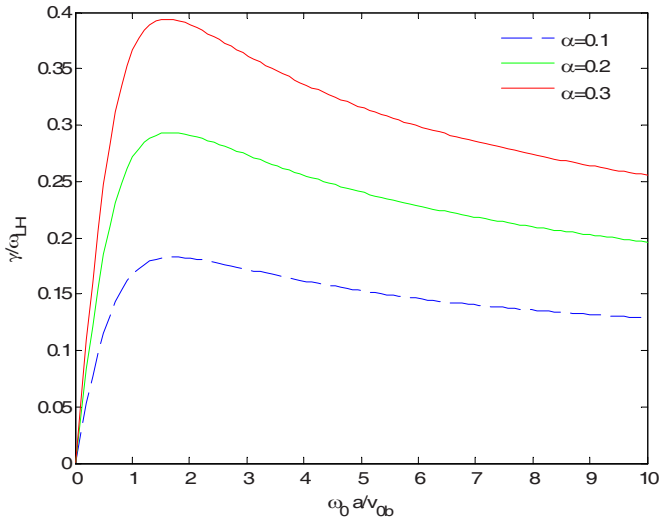

FIG. 5. (Color online) Normalized growth rate with normalized beam velocity for different magnetic shear parameters $\alpha=0.1$, $\alpha=0.2$, and $\alpha=0.3$.

III. RESULTS AND DISCUSSION

In order to have a numerical appreciation of results we consider the following set of parameters, corresponding to W7-AS[6]: Electron density (of a hydrogen plasma) $\approx(2-6)\times10^{13}$ cm^{-3}, electron temperature 1–1.2 keV, ion temperature 600–900 eV, magnetic field 2.5 T. The total power of the hydrogen beam is about 600 kW and the density at the stationary phase $\approx(2-4)\times10^{-2}n_0$.

In Fig. 3, we have plotted the lower hybrid wave dispersion relation for various values of shear parameter. For a particular value of $k_y a$ eigenfrequency of the lower hybrid wave increases significantly with the increase of the shear parameter. In the same figure we also plotted the Cerenkov resonance condition $\omega=k_y v_{ob}$ (beam mode). The intersection point of the dispersion curve and the beam mode gives the

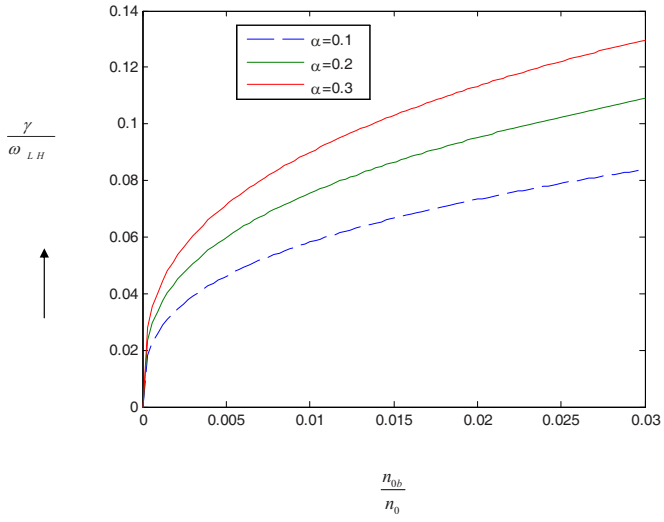

FIG. 6. (Color online) Normalized growth rate as a function of normalized beam density with plasma density $\sim(2-6)\times10^{13}$ cm^{-3} and beam density $\sim(2-4)\times10^{-2}n_0$, for different magnetic shear parameter $\alpha=0.1$, $\alpha=0.2$, and $\alpha=0.3$.

frequency of the unstable lower hybrid eigenmode. This frequency increases with the beam velocity (or beam energy).

The mode structure of the lower hybrid mode (cf. Fig. 4) is evanescent in the inner and outer regions while propagating waves in the intermediate region, which is quite similar to the experimental observation by Shalashov *et al.*[6]

In Fig. 5 we have plotted the normalized growth rate of the instability as a function of normalized frequency for different values of the sheared parameter, $\alpha=0.1$, 0.2, and 0.3. The growth rate initially rises with the frequency, attains a maximum around $\omega \simeq 2v_{0b}/a$, and then falls off gradually. With increasing shear parameter, the growth rate increases.

In Fig. 6 we have plotted the normalized growth rate of the instability as a function of normalized beam density for the same parameter as given above. It can be seen that the growth rate increases with the beam density similar to the experimental observation made by Shalashov *et al.*[6] and Chang.[8] However, Chang's case is quite different. He is studying the growth of the negative energy lower hybrid mode (modified by the ion beam) due to the Landau damping introduced by the electrons. As the electrons take away energy from the negative energy mode, its energy becomes more negative, i.e., the amplitude of the mode increases. In our present case we are dealing with a sort of two stream instability where the ion beam resonantly interacts with a positive energy lower hybrid mode via the Cerenkov interaction. The growth rate scales as $\gamma \sim n_{0b}^{1/3}$.

In Rosenberg[22] and Chang's[8] prediction, there is no variation of the shear parameter, i.e., $\alpha=0$, so the parallel wave number is constant, but with the variation of the shear parameter (α), the parallel wave number changes the localized modes in the intermediate region.

ACKNOWLEDGMENTS

The authors would like to thank Professor D. J. Campbell and Professor Toshihiro Oikawa of the Fusion Science and Technology Department, ITER Organization, CEA Cadarache Centre, France, and the referee for his constructive comments.

[1] M. Seki, M. Saigusa, M. Nemoto, K. Kusama, T. Tobita, M. Kuriyama, and K. Uehara, Phys. Rev. Lett. **62**, 1989 (1989).
[2] G. A. Cottrel and R. O. Dendy, Phys. Rev. Lett. **60**, 33 (1988).
[3] P. Schild, G. A. Cottrell, and R. O. Dendy, Nucl. Fusion **29**, 834 (1989).
[4] The JET Team, Nucl. Fusion **32**, 187 (1992).
[5] G. A. Cottrel, V. P. Bhatnagar, O. Da Casta, R. O. Dendy, J. Jacquinot, K. G. McClements, D. C. McCune, M. F. F. Nave, P. Smeulders, and D. F. H. Start, Nucl. Fusion **33**, 1365 (1993).
[6] A. G. Shalashov, E. V. Suvarov, L. V. Lubyako, H. Maassberg, and the W7–AS Team, Plasma Phys. Controlled Fusion **45**, 395 (2003).
[7] G. J. Greene and the TFTR Team, *Proceedings of the 17th European Conference on Controlled Fusion and Plasma Heating* (European Physical Society, Petit-Lancy, 1990), p. 1540.
[8] R. P. H. Chang, Phys. Rev. Lett. **35**, 285 (1975).
[9] R. P. H. Chang and M. Porkolab, Nucl. Fusion **16**, 142 (1976).
[10] A. P. H. Goede, P. Massmann, H. J. Hopman, and J. Kistemaker, Nucl. Fusion **16**, 85 (1976).
[11] D. K. Bhadra, S. C. Chiu, D. Buchenauer, and D. Hwang, Nucl. Fusion **26**, 201 (1986).
[12] J. Baldzuhn, A. Werner, H. Wobig, N. Rust, S. Klose, and W7-AS Team, Plasma Phys. Controlled Fusion **45**, 891 (2003).
[13] ITER Physics Expert Group on Energetic Particles, Nucl. Fusion **39**, 2495 (1999).
[14] K. Nagaoka, M. Yokoyama, Y. Takeiri *et al.*, J. Plasma Fusion Res. **1**, 1 (2006).
[15] K. Mc Gurie, R. Goldston, M. Bell *et al.*, Phys. Rev. Lett. **50**, 891 (1983).
[16] W. W. Heidbrink, K. Bol, D. Buchenauer *et al.*, Phys. Rev. Lett. **57**, 835 (1986).
[17] J. D. Strachan, B. Grek, W. Heidbrink *et al.*, Nucl. Fusion **25**, 863 (1985).
[18] L. Chen, R. B. White, and M. N. Rosenbluth, Phys. Rev. Lett. **52**, 1122 (1984).
[19] R. B. White, L. Chen, F. Romanelli, and R. Hay, Phys. Fluids **31**, 1630 (1988).
[20] B. Coppi and F. Porcelli, Phys. Rev. Lett. **57**, 2272 (1986).
[21] D. Zhou, Phys. Plasmas **13**, 072511 (2006).
[22] M. Rosenberg, M. Salimullah, and R. Bharuthram, Planet. Space Sci. **47**, 1517 (1999).
[23] S. Sen and R. A. Cairns, Phys. Plasmas **7**, 2939 (2000).
[24] X. Y. Fu, J. Q. Dong, W. Horton, C. T. Ying, and G. J. Liu, Phys. Plasmas **4**, 588 (1997).
[25] M. Uchida, S. Sen, and A. Fukuyama, Phys. Plasmas **10**, 4758 (2003).
[26] S. Sen, R. A. Cairns, and R. G. Storer, Phys. Plasmas **7**, 1192 (2000).
[27] C. S. Liu and V. K. Tripathi, Phys. Plasmas **3**, 3410 (1996).